JOURNAL

OF THE AMERICAN CHEMICAL SOCIETY

VOLUME 110, NUMBER 17 AUGUST 17, 1988

Matrix Reactions of Oxygen Atoms with P_4. Infrared Spectra of P_4O, P_2O, PO, and PO_2

Lester Andrews* and Robert Withnall

Contribution from the Chemistry Department, University of Virginia, Charlottesville, Virginia 22901. *Received November 10, 1987*

Abstract: Oxygen atoms (^{16}O and ^{18}O) from ozone photolysis and discharge of oxygen molecules were reacted with P_4 molecules and the products were trapped in solid argon at 12 K. The major product P_4O exhibited a strong terminal P=O stretching mode at 1241 cm^{-1}, a P—P=O deformation mode at 243 cm^{-1}, and four P–P stretching modes near P_4 values, all of which characterize a C_{3v} species. Two new molecular species probably arise from energized P_4O before relaxation by the matrix: The first absorbed at 1197 cm^{-1}, photolyzed with red light, and is probably P_2O. The second absorbed at 856 and 553 cm^{-1}, increased with short-wavelength radiation, and is most likely due to the C_{2v} bridge-bonded P_4O structural isomer. Higher discharge power gave O atoms and vacuum ultraviolet radiation; these conditions favored the bridge-bonded P_4O species and the simple oxides PO and PO_2, which were observed at 1218 and 1319 cm^{-1}, respectively. The matrix efficiently quenched the large exothermicity (130 ± 10 kcal/mol) for the P_4 + O reaction and allowed the lowest oxide of phosphorus, P_4O, to be trapped for the first time as a molecular species.

The oxidation of phosphorus has been an important chemical problem since the discovery of this reaction by Robert Boyle in 1680. A large number of stable chemical species are produced, owing to the several oxidation states of phosphorus and the strong phosphorus–oxygen bonds that can be formed.[1] The greenish glow observed on oxidation of white phosphorus has fostered extensive studies aimed at identifying the emitting oxide species.[2-7] Although the PO diatomic[8-11] and PO_2 triatomic[12-14] molecules have been studied extensively, the less stable lower oxidation state species P_4O and P_2O have not been characterized. The matrix isolation technique is particularly well suited for quenching internal energy and stabilizing transient species that react further in the gas phase. Accordingly, matrix reactions of P_4 and O atoms have been performed with the aim of trapping the lowest oxides of phosphorus for spectroscopic study.

Experimental Section

The CTI Cryogenics Model 22 cryocooler, Perkin-Elmer 983 spectrometer, photolysis lamps, and vacuum apparatus have been described previously.[15-18] Spectra presented here were processed by subtracting a background spectrum of the cold CsI window and by base-line correction to compensate for matrix light scattering. Frequency accuracy is ±0.5 cm^{-1}. The method for preparing and handling ozone and isotopic ozones has been detailed in earlier reports.[16,18] The basic problem here was maintaining the optimum effusion rate of P_4, and many of the 32 experiments performed had excessive P_4 and no infrared transmission. Although several delivery methods were used, including the flow of argon over P_4 in a glass trap at 0 °C, the best technique was to cut small pieces (3 mm)^3 of white phosphorus in a glovebag under argon and place the element in a glass tube behind a Teflon needle valve (Ace Glass). The evaporation rate of P_4 directly into the matrix for 6–12 h was controlled by the needle valve and monitored by the infrared spectrum. A 6-mm-o.d. quartz tube was used to direct the flow of discharged argon/oxygen (generally 50/1) onto the 12 K cold window. Two different microwave discharge (Evenson-Broida cavity, Burdick Model MW 200, 375 W diathermy) conditions were employed: The first experiments employed low microwave power (20–30%) and just maintained the discharge in the back of the quartz tube. The second studies used high microwave power (70–80%), and the discharge glow reached the tube orifice 2 cm from the cold window.

Results

Three different types of experiments will be described where P_4 vapor was codeposited with argon at 12 K and reacted with

(1) Mellor, J. W. *Inorganic and Theoretical Chemistry*; Wiley-Interscience: New York, 1971; Vol. VIII, Supp. III. Phosphorus, Chapters IV and V.
(2) Davies, P. B.; Thrush, B. A. *Proc. R. Soc. London, A* **1968**, *302*, 243.
(3) Van Zee, R. J.; Khan, A. U. *J. Phys. Chem.* **1976**, *65*, 764; *J. Phys. Chem.* **1976**, *80*, 2240.
(4) Fraser, M. E.; Stedman, D. H. *J. Chem. Soc., Faraday Trans. 1* **1983**, *79*, 527; **1984**, *80*, 285.
(5) Hamilton, P. A.; Murrells, T. P. *J. Chem. Soc., Faraday Trans. 2* **1985**, *81*, 1531; *J. Phys. Chem.* **1986**, *90*, 182.
(6) Harris, D. G.; Chou, M. S.; Cool, Ta. A. *J. Chem. Phys.* **1985**, *82*, 3502.
(7) Lohr, L. L. *J. Phys. Chem.* **1984**, *88*, 5569.
(8) Ngo, T. A.; DaPaz, M.; Coquart, B.; Couet, C. *Can. J. Phys.* **1974**, *52*, 154.
(9) Ghosh, S. N.; Verma, R. D. *J. Mol. Spectrosc.* **1978**, *72*, 200.
(10) Larzilliere, M.; Jacox, M. E. *NBS Spec. Publ. (U.S.)* **1979**, *561*, 529; *J. Mol. Spectrosc.* **1980**, *79*, 132.
(11) Kawaguchi, K.; Saito, S.; Hirota, E.; Ohashi, N. *J. Chem. Phys.* **1983**, *79*, 829.
(12) Verma, R. D.; McCarthy, C. F. *Can. J. Phys.* **1983**, *61*, 1149.
(13) Kawaguchi, K.; Saito, S.; Hirota, E.; Ohashi, N. *J. Chem. Phys.* **1985**, *82*, 4893.
(14) Hamilton, P. A. *J. Chem. Phys.* **1987**, *86*, 33.
(15) Andrews, L. *J. Chem. Phys.* **1971**, *54*, 4935.
(16) Andrews, L.; Spiker, R. C., Jr. *J. Phys. Chem.* **1972**, *76*, 3208.
(17) Kelsall, B. J.; Andrews, L. *J. Chem. Phys.* **1982**, *76*, 5005.
(18) Withnall, R.; Hawkins, M.; Andrews, L. *J. Phys. Chem.* **1986**, *90*, 575.

0002-7863/88/1510-5605$01.50/0

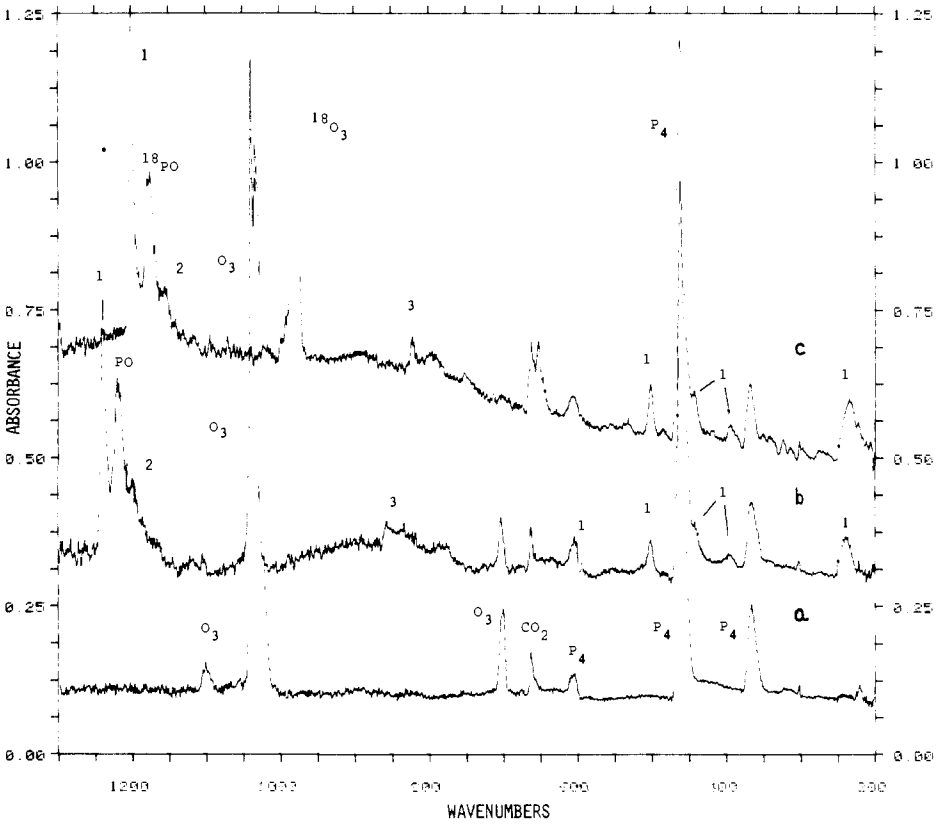

Figure 1. Infrared spectra of P_4 and O_3 in solid argon at 12 K: (a) P_4 vapor codeposited with 24 mmol of $Ar/O_3 = 150/1$ sample for 6 h; (b) after photolysis at 520–1000 nm for 20 min; (c) P_4 vapor codeposited with 26 mmol of $Ar/^{18}O_3 = 150/1$ sample for 9 h and after 520–1000-nm photolysis for 20 min.

oxygen atoms. Infrared spectra revealed the P_4 bands illustrated in Figure 1a: a very strong ν_3 (F_2) band at 461 cm^{-1} with a 465-cm^{-1} shoulder, a medium ν_2 (E) band at 370 cm^{-1} with a 365-cm^{-1} shoulder, a weak sharp ν_1 (A_1) band at 610 cm^{-1}, and a weaker $2\nu_3$ band at 915 cm^{-1}. These bands are in agreement with a preliminary matrix infrared spectrum[19] and infrared and Raman spectra of P_4 vapor and solutions[20] where the lowered symmetry of P_4 in solution makes the ν_1 (A_1) and ν_2 (E) bands observable in the infrared spectrum.

P_4 and O_3. P_4 vapor was codeposited with an $Ar/O_3 = 150/1$ mixture on a 12 K window, and the spectrum in Figure 1a shows the P_4 and O_3 fundamentals.[16,18-20] Although no evidence was found for reaction between P_4 and O_3 during deposition, the reagent fundamentals were broadened, ν_1 and ν_2 of P_4 were shifted to 604 and 367 cm^{-1}, respectively, and ν_1 and ν_2 of O_3 were shifted to 1100 and 700 cm^{-1}. The sample was photolyzed by the 590–1000-nm output of a high-pressure mercury arc for 20 min, and new bands appeared in the spectrum at 1241 (**1**), 1197 (**2**), 856

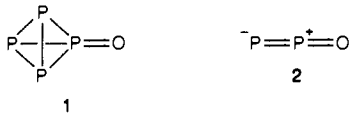

1

2

cm^{-1} (**3**), 501, 441, 393, and 243 cm^{-1} (labeled **1** in Figure 1b),

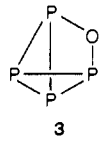

3

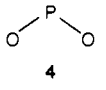

4

and 1218 cm^{-1} (PO),[10] while O_3 and P_4 bands were reduced by 30%. Continued irradiation at 520–1000 nm for 20 min more reduced reagent bands about 10% more, reduced the 1197-cm^{-1} band by half, doubled the PO and **1** product bands, and increased the weak new band at 856 cm^{-1} (**3**); this spectrum is shown in Figure 1b. A sharp new 603-cm^{-1} band was observed on top of the broader P_4 absorption at 604 cm^{-1}. A final 220–1000-nm irradiation reduced the ozone bands slightly, left the **1** bands unchanged, destroyed the 1197-cm^{-1} and PO bands, increased the 856-cm^{-1} band 3-fold, and produced a weak new associated 553-cm^{-1} band. An analogous experiment was done with $^{18}O_3$, and the results were similar; the band positions are compared in

Table I. Infrared Absorptions (cm^{-1}) Observed in P_4 and O_3 Codeposition and Photolysis Experiments

		photolysis[a]			
$^{16}O_3$	$^{18}O_3$	590 nm	520 nm	220 nm	indent
1241	1202	p	i	p	P_4O (ν_1) (A_1)[b]
1218	1173	p	i	d	PO[c]
1197	1153	p	d	d	P_2O
1119	1070	–	p	i	?
1100	1040	d	d	d	P_4--O_3
1040	883	d	d	d	O_3 (ν_3)
856	822	p	i	i	P_4O bridged
700	664	d	d	d	P_4--O_3
604	604	x	x	x	P_4--O_3
603	603	p	i	–	P_4O (ν_2) (A_1)[b]
553	533	–	–	p	P_4O bridged
501	501	p	i	–	P_4O (ν_4) (E)[b]
461	461	d	d	–	P_4 (ν_3)
441	441	p	i	–	P_4O (ν_3) (A_1)[b]
393	393	p	i	–	P_4O (ν_5) (E)[b]
367	367	d	d	–	P_4--O_3
243	237	p	i	–	P_4O (ν_6) (E)[b]

[a] Photolysis notation: p denotes produced, – indicates no change, i indicates increase, d denotes decrease, and x indicates unknown. [b] Terminally bonded P_4O with C_{3v} structure. [c] Perturbed site also observed at 1222 cm^{-1} owing to the presence of photolysis byproducts in the matrix cage.

(19) Boyle, M. E.; Williamson, B. E.; Schatz, P. N.; Marks, J. P.; Snyder, P. A. *Chem. Phys. Lett.* **1986**, *125*, 349.
(20) Gutowsky, H. S.; Hoffman, C. J. *J. Am. Chem. Soc.* **1950**, *72*, 5751.
(21) Bosworth, Y. M.; Clark, R. J. H.; Rippon, D. M. *J. Mol. Spectrosc.* **1973**, *46*, 240.

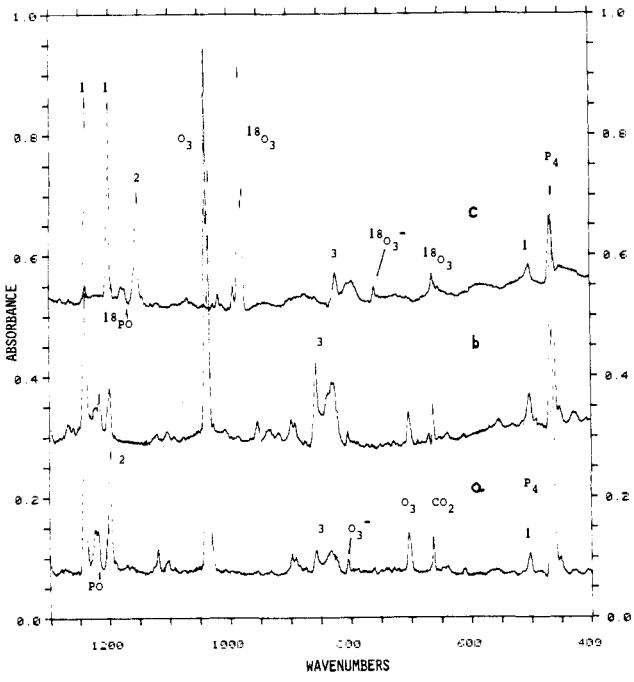

Figure 2. Infrared spectra of P_4 and O atom reaction products in solid argon at 12 K: (a) P_4 vapor codeposited with 38 mmol of Ar/O_2 = 50/1 sample passed through low-power microwave discharge for 12 h; (b) spectrum after full medium-pressure mercury arc photolysis; (c) P_4 vapor codeposited with 16 mmol of $Ar/^{18}O_2$ = 50/1 sample subjected to low-power discharge for 6 h.

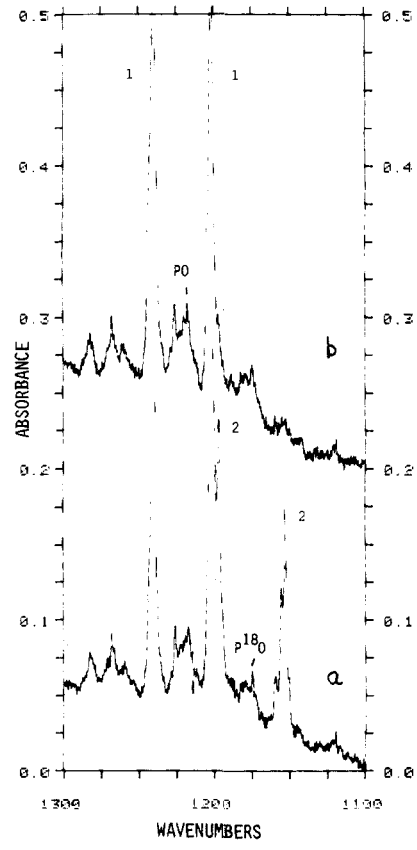

Figure 3. Infrared spectra of P_4 and isotopic O atom matrix reaction products in the 1100–1300-cm^{-1} region: (a) P_4 vapor codeposited with 22 mmol of $Ar/^{16,18}O_2$ = 50/1 sample passed through low-power discharge for 12 h; (b) after 520–1000-nm photolysis for 20 min.

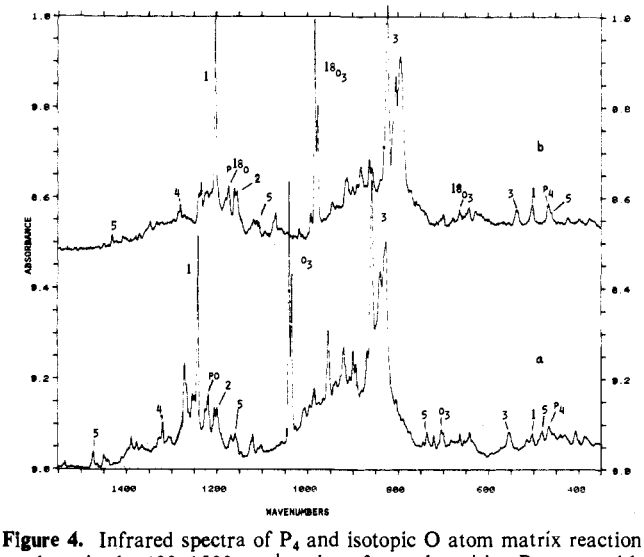

Figure 4. Infrared spectra of P_4 and isotopic O atom matrix reaction products in the 400–1500-cm^{-1} region after codepositing P_4 vapor with 15 mmol of Ar/O_2 = 50/1 sample passed through a high-power microwave discharge: (a) $^{16}O_2$ for 7 h; (b) $^{18}O_2$ for 9 h.

Table I for the isotopic ozone experiments. Again, 590-nm photolysis produced the new bands, and 520-nm irradiation doubled all but the **2** band at 1154 cm^{-1}, which was halved; this spectrum is shown in Figure 1c. The final 220–1000-nm photolysis destroyed the $P^{18}O$ and **2** bands, left **1** absorptions unchanged, and tripled **3** bands.

P_4 and O Atoms. The first series of P_4 codeposition experiments with an Ar/O_2 stream subjected to low-power microwave discharge exhibited half as much P_4 as the ozone experiments and a small amount of ozone in the original spectrum, Figure 2a, of the deposited sample. In addition, the **1** and **3** bands were observed with intensity similar to that in Figure 1b, the 1197-cm^{-1} band (**2**) was 1 order of magnitude stronger, and a weak isolated ozonide[22] band was observed at 804.3 cm^{-1}. Photolysis by the full light of a medium-pressure arc for 1 h increased the **1** bands by 20%, increased the **3** bands 4-fold, reduced the 1197-cm^{-1} band by 70%, decreased the O_3^- band by 20%, increased the sharp PO band at 1218 cm^{-1} at the expense of the shoulder at 1222 cm^{-1}, and produced weak new bands at 952 and 919 cm^{-1} as is illustrated in Figure 2b. An analogous experiment with $^{18}O_2$ produced the spectrum shown in Figure 2c where isotopic shifts for all of the product bands can be ascertained. Another experiment was done with $^{16,18}O_2$ in the discharged argon stream. The product spectrum revealed the same bands as the ^{16}O and ^{18}O reactions separately. Figure 3a shows the intense sharp **1** doublet at 1240.9 and 1202.4 cm^{-1}, the medium **2** doublet at 1197.3 and 1153.4 cm^{-1}, and the weak sharp PO doublet at 1218.3 and 1173.1 cm^{-1}, which characterize vibrations of species containing a single O atom. Irradiation at 590 nm reduced the **2** doublet by 70%, increased **1** bands by 30%, and left P_4, O_3, and 856-cm^{-1} bands unchanged. Photolysis at 520 nm continued this trend, as shown in Figure 3b, and increased the **3** doublet at 856 and 822 cm^{-1} and the associated 553- and 536-cm^{-1} doublet by 20%. Full-arc radiation produced broad PO and $P^{18}O$ bands, increased the **3** doublets by 100%, and revealed new isotopic components on the 1270-cm^{-1} band.

The second series of P_4 reactions with Ar/O_2 subjected to high-power microwave discharge consumed much more P_4 than the low-power discharge experiments as is shown in Figure 4. The most striking differences between high- and low-power discharge experiments are the reduced yield of species **2** and isolated O_3^- and the much larger yield of species **3** and other new absorptions with the high-power discharge. Additional bands were observed at 1319 cm^{-1} (**4**) and 1472, 1158, 735, and 479 cm^{-1} (**5**), which have been observed in previous PH_3 + O studies,[23] and sharp new absorptions appeared at 952, 919, and 898 cm^{-1}. Bands observed in the discharge experiments with $^{16}O_2$ and $^{18}O_2$ are given in Table

(22) Andrews, L.; Ault, B. S.; Grzybowski, J. M.; Allen, R. O. *J. Chem. Phys.* **1975**, *62*, 2461.

(23) Withnall, R.; Andrews, L. *J. Phys. Chem.* **1988**, *92*.

Table II. Infrared Absorptions (cm^{-1}) Observed in Experiments Codepositing P_4 Vapor with Ar/O_2 Stream Passed through High-Power Microwave Discharge onto CsI Window at 12 K

$^{16}O_2$	$^{18}O_2$	$^{16,18}O_2$	ident
1536	1450	3[a]	O_2^--P_xO_y complex
1473	1431		P_2O_5
1449 w	1408		$HOPO_2$
1389 w	1380		HO_2
1319.1	1280.2	3[a]	PO_2 (4)
1270	1233	4[b]	P_xO_y
1254			
1240.9	1202.5	2	P_4O (1) terminal
1218.3	1173.1	2	PO
1204 w	1160	2	X--PO
1198 w	1154 w	2	P_2O (2)
1168 w	1118		?
1158	1105		P_2O_5
1119	1070		?
1040	883		O_3
952	913	4[c]	P_xO_y
919	881		P_xO_y
898	861		P_xO_y
856	822		P_4O (3) bridged
838	803	2	site
827	793		site
735	703		P_2O_5
641	626		P_xO_y
553	536	2	P_4O (3) bridged
501	501		P_4O (1) terminal
479	459		P_2O_5
465	465		P_4
405			P_xO_y

[a] Number of components in isotopic multiplet with $^{16,18}O_2$. [b] Isotopic multiplet at 1270, 1265, 1238, and 1233 cm^{-1}. [c] Isotopic multiplet at 952, 936, 922, and 913 cm^{-1}.

II. A final experiment was done with $^{16,18}O_2$, and the **1**–**3** and PO product species gave the same spectra as in the $^{16}O_2$ and $^{18}O_2$ studies without new intermediate components. The 900- and 1300-cm^{-1} regions, however, revealed new mixed isotopic components. Figure 5 compares the isotopic absorptions in the 1300-cm^{-1} region. The 1319.1-cm^{-1} band produced with $^{16}O_2$ in Figure 5a shifted to 1280.2 cm^{-1} with $^{18}O_2$ (Figure 5c) and yielded a 1/2/1 relative intensity triplet with a central component at 1301.4 cm^{-1} (Figure 5b). Figure 6 illustrates the 1330–1140-cm^{-1} region with $^{16,18}O_2$; the **4** triplet, a 1270–1233-cm^{-1} multiplet, the strong **1** doublet, and sharp PO and **2** doublets were observed.

Discussion

The new binary phosphorus–oxygen molecular species produced in the present argon matrix reactions of the elements will be identified, and the reaction mechanisms will be proposed.

PO and P_2O_5. The sharp 1218.3-cm^{-1} band and ^{18}O counterpart at 1173.1 cm^{-1} are in excellent agreement with the previous matrix assignment to PO and $P^{18}O$ in solid argon;[10] the matrix 1218.3-cm^{-1} band is red shifted 2 cm^{-1} from the gas-phase ground-state fundamental.[8] The weak 1473-, 1158-, 735-, and 479-cm^{-1} bands (**5**) in the high-power discharge experiment with $^{16}O_2$ agree with stronger bands from the parallel PH_3 + O study. The 1158-cm^{-1} band exhibited a triplet of triplets with $^{16,18}O_2$ for a vibration involving two equivalent PO_2 groups each with equivalent O atoms, and the 735-cm^{-1} absorption exhibited the proper ^{18}O shift for an antisymmetric P–O–P vibration, which provide the molecular P_2O_5 identification for these absorptions.[23] The sharp P_2O_5 bands were observed here only in the high-power discharge experiments, which provided increased yields of O atoms and intense vacuum ultraviolet light in the region of P_4 absorptions.[19] This radiation may foster more reaction or dissociation of P_4 and give more higher phosphorus oxide species than observed in the low-power discharge experiments.

PO_2. The sharp 1319.1-cm^{-1} species **4** band was also observed in previous matrix studies using PH_3 and PD_3 as sources of phosphorus atoms,[10,23] and its assignment to ν_3 of PO_2 was suggested.[23] The present isotopic observations verify the PO_2 identification. First, the ν_3 mode is alone in the B_2 symmetry class,

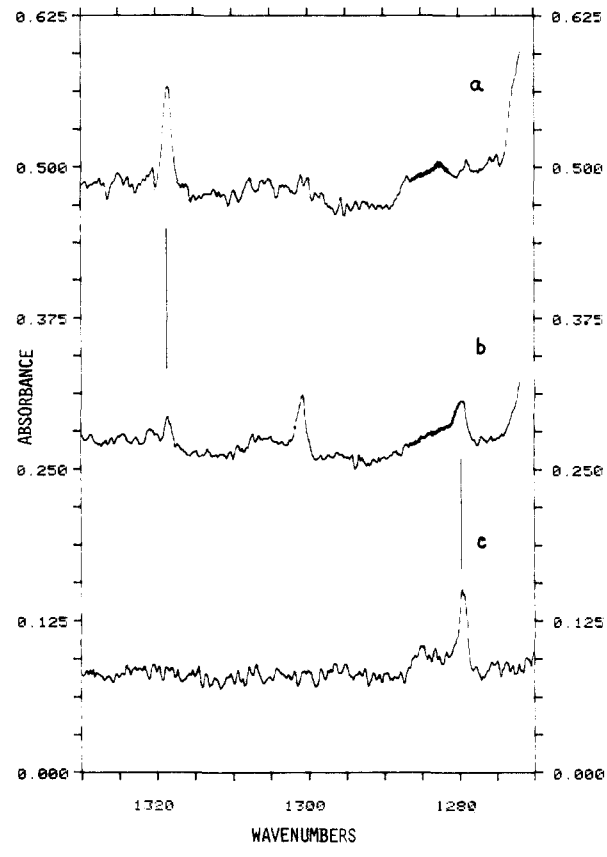

Figure 5. Infrared spectra of P_4 and isotopic O atom matrix reaction products in the 1270–1330-cm^{-1} region using high-power discharge of 15 mmol of Ar/isotopic O_2 = 50/1 samples for 5–9 h: (a) $^{16}O_2$; (b) $^{16,18}O_2$, 55% ^{18}O enrichment; (c) $^{18}O_2$, 98% ^{18}O enrichment.

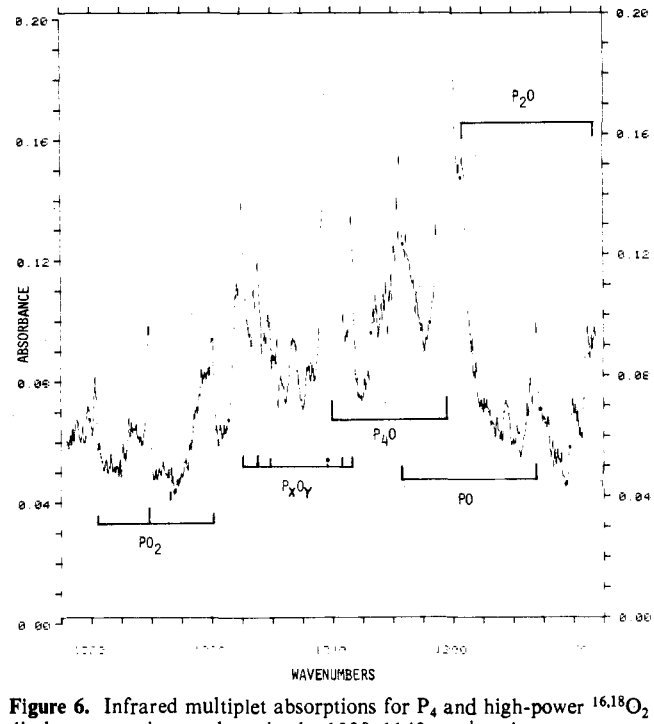

Figure 6. Infrared multiplet absorptions for P_4 and high-power $^{16,18}O_2$ discharge reaction products in the 1330–1140-cm^{-1} region.

and when the 135.3° bond angle from the microwave study is used,[13] the ν_3 fundamental for $P^{18}O_2$ is predicted at 1279.6 cm^{-1}, just 0.6 cm^{-1} below the observed value. This small deviation is of the magnitude expected for calculations using the harmonic approximation on account of small anharmonic terms in the potential function. Second, the 1/2/1 relative intensity triplet (Figure 5b) using discharged $^{16,18}O_2$ clearly demonstrates the involvement

of two equivalent oxygen atoms in this vibration. Third, PO_2 was favored in the high-power discharge experiments, which provided vacuum ultraviolet photolysis of the sample. The extra radiation destroyed any isolated O_3^- formed and made it similarly unlikely that any PO_2^- could be trapped. This fact and the observation of PO_2^- somewhat lower[24] in solid KCl at 1207 cm^{-1} rule out PO_2^- as the origin of the 1319-cm^{-1} band. Fourth, centrifugal distortion constants from the microwave spectrum of PO_2 predict the harmonic ν_3 fundamental in the (1300 ± 100)-cm^{-1} region.[13] Fifth, ab initio calculations[7] scaled against PO predict ν_3 of PO_2 near 1260 cm^{-1}. Finally, the 2-cm^{-1} matrix shift for PO suggests that ν_3 of PO_2 in the gas phase will be observed in the (1320 ± 10)-cm^{-1} region.

Note Added in Proof. $Neon/O_2/PCl_3$ mixtures heated to 1200 °C and then condensed at 4 K revealed a new 1320.4-cm^{-1} absorption, which is appropriate for PO_2 (Bondybey, V. E., unpublished results).

Terminally Bonded P_4O. The bands labeled **1** were favored in P_4--O_3 photolysis and low-power O_2 discharge experiments These bands include a strong, sharp 1240.9-cm^{-1} band and a weak 243-cm^{-1} band that show large ^{18}O shifts and 603-, 501-, 441-, and 393-cm^{-1} bands that exhibit no ^{18}O shift and are near P_4 fundamentals. The **1** bands are assigned to the P_4O molecule, which is thereby characterized as a C_{3v} species with some similarities to the H_3PO molecule. These molecules have three symmetric (A_1) and three antisymmetric (E) vibrational modes, and the normal modes of molecular P_4O will be assigned accordingly. The "P=O" stretch of H_3PO was observed at 1240.2 cm^{-1}, but this band showed a PD_3 shift owing to mixing with the symmetric PH_3 deformation mode.[25] The 1241-cm^{-1} band is assigned to ν_1 (A_1), the symmetric terminal P=O stretching mode. A harmonic diatomic calculation predicts the ^{18}O counterpart at 1194 cm^{-1}, below the observed value of 1202 cm^{-1}. This discrepancy suggests slight mixing with another symmetric mode in this region. Since there is no other A_1 fundamental nearby, a Fermi resonance type of interaction is probably involved. For P_4 itself, $2 \times \nu_3 =$ 922 cm^{-1}, and the $2\nu_3$ overtone was observed at 915 cm^{-1}. If a similar anharmonicity is present in the 603-cm^{-1} ν_2 fundamental for P_4O, then $2\nu_2$ for P_4O is predicted near 1190 cm^{-1}. For $P_4{}^{18}O$ the ν_1 fundamental predicted at 1194 cm^{-1} would interact with $2\nu_2$ and be shifted up (to 1202 cm^{-1}) while $2\nu_2$ would be shifted down a comparable amount. Unfortunately, the region for $2\nu_2$ is complicated by other absorptions, and no evidence was found for the overtone band of either isotope.

The ν_2 (A_1) mode at 603 cm^{-1} involves symmetric stretching of the P_4 tetrahedron, which was observed for P_4 at 610 cm^{-1}. The triply degenerate antisymmetric P–P stretching mode of P_4 at 461 cm^{-1} is split into A_1 and E modes in P_4O; presumably, the stronger 501-cm^{-1} band is ν_4 (E) and the weaker 441-cm^{-1} band is ν_3 (A_1). The doubly degenerate 370-cm^{-1} stretching mode for P_4 exhibits a P_4O counterpart at 393 cm^{-1}, which is assigned to ν_5 (E). The final 243-cm^{-1} band is assigned to the doubly degenerate P—P=O deformation mode ν_6 (E), which appears at 333 cm^{-1} for $Cl_3P^{16}O$ and 323 cm^{-1} for $Cl_3P^{18}O$.[26] The ^{18}O shift to 237 cm^{-1} shows that the 243-cm^{-1} vibration is primarily an oxygen motion.

The lowest oxide of phosphorus, P_4O, is photochemically stable as was found for H_3PO as well.[25] This is expected since P_4 absorbs only in the vacuum ultraviolet region.[19] Finally, the four P_4 subgroup modes in P_4O exhibit a small (average 10-cm^{-1}) increase over isolated P_4 values; this suggests that the effect of oxygen in P_4O may be to slightly reduce the P–P bond lengths in the P_4 subgroup.

P_2O. The sharp 1197.3-cm^{-1} band (**2**) was weak after 590-nm photolysis of P_4--O_3 samples, which is expected since 590-nm radiation markedly decreased the medium-intensity 1197.3-cm^{-1} band produced in the low-power discharge experiments. The 1197.3-cm^{-1} band is due to an almost pure P=O stretching mode; a harmonic diatomic calculation predicts the ^{18}O counterpart at 1152.6 cm^{-1}, just 0.8 cm^{-1} below the observed value. Although no other fundamental could be detected for the single O atom species absorbing at 1197.3 cm^{-1}, it is probably due to the simple P_2O molecule for the following reasons. The example of N_2O, which photodissociates with hard-ultraviolet radiation,[27] suggests that P_2O should photolyze at longer wavelengths. This is further justified by the relatively weaker P_2 diatomic bond (117 ± 1 kcal/mol).[1] It is suggested that P_2O dissociates readily to P and PO in contrast to N_2O, which gives N_2 and O. In support of the observation of P_2O from the P_4 + O matrix reaction, the P_2O molecule has been detected by mass spectroscopy from the same gas-phase reaction.[28] Mechanistic evidence, namely the predicted 130 ± 10 kcal/mol exothermicity of the P_4 + O reaction and the 55 kcal/mol dissociation energy of P_4 into P_2 molecules,[1] suggests that P_2 and P_2O are secondary products of the P_4 + O reaction. This proposal is supported by the 590-nm photodissociation of P_2O, although a photoinduced reaction between P_2O and P_2 in the same matrix cage to reproduce P_4O cannot be ruled out, and by UV photolysis to give PO in the low-power discharge experiments.

Bridge-Bonded P_4O. Another major product (**3**) in these experiments grows on short-wavelength photolysis in contrast to terminally bound P_4O, which is not changed. This product is favored relative to terminal P_4O in high-powered discharge experiments and exhibits strong, sharp 856-cm^{-1} and sharp, weak 553-cm^{-1} absorptions. These bands shift to 882 and 536 cm^{-1} with ^{18}O, and mixed $^{16,18}O$ experiments produced doublets with no evidence for mixed isotopic absorptions. The weaker absorption at 553 cm^{-1} is associated with the stronger 856-cm^{-1} absorption based on a 13 ± 2 absorbance ratio for the two bands in five different discharge experiments and their parallel growth on photolysis. Vibrational spectra[29] of P_4O_6, which contains oxygen atoms bridge-bonded between phosphorus atoms, reveal the strongest antisymmetric P–O–P stretching mode at 953 cm^{-1} and the symmetric stretching mode at 640 cm^{-1} in solid argon. The 856- and 553-cm^{-1} bands fall just below these characteristic P_4O_6 modes, which suggests their consideration for a bridged P_4O species with C_{2v} symmetry.

The P–O–P angle is 126° in P_4O_6; however, insertion of oxygen in only one edge of the P_4 tetrahedron results in a somewhat smaller P–O–P angle, owing to shorter P–P distances[30] in P_4 as compared to P_4O_6. Only approximate vibrational calculations can be done for the bridged P_4O species, owing to lack of data, and the P–O–P subgroup will be treated separately as an approximation. The ^{18}O shifts observed for the stronger antisymmetric and weaker symmetric stretching modes are 34 and 17 cm^{-1}, respectively. Assuming a P–O–P angle of 126°, approximate shifts of 36.7 and 13.9 cm^{-1} are predicted. Shifts of 36.5 and 15.3 cm^{-1} are predicted for 120°, 35.0 and 17.5 cm^{-1} for 110°, 33.7 and 19.4 cm^{-1} for 100°, and 32.0 and 20.6 cm^{-1} for 90° (same as diatomic molecule). Considering the approximations involved, the agreement (within 1 cm^{-1}) at 110° is very good. This estimated P–O–P bond angle and the 1.64-Å P–O distance in P_4O_6 give a P–P separation of 2.68 Å along the edge of the P_4 tetrahedron inserted by oxygen. This, of course, is less than the P_4O_6 value (2.92 Å) and greater than the P_4 dimension (2.21 Å).[30] These arguments are consistent with identification of species **3** as a bridge-bonded P_4O species, clearly a structural isomer of the terminally bonded species **1**. Species **3** is analogous to H_2POH, a structural isomer of H_3PO in the similar PH_3 plus oxygen atom system.[25]

Other Species. The weaker 952-, 919-, 898-, and 1270-cm^{-1} bands were favored by the high-power discharge and showed large ^{18}O shifts, and they are probably due to higher phosphorus oxide

(24) Hunter, S. J.; Hipps, K. W.; Francis, A. H. *Chem. Phys.* **1979**, *39*, 209.
(25) Withnall, R.; Andrews, L. *J. Phys. Chem.* **1987**, *91*, 784.
(26) Moores, B.; Andrews, L., to be submitted for publication.
(27) Herzberg, G. *Electronic Spectra and Electronic Structure of Polyatomic Molecules*; Van Nostrand: Princeton, NJ, 1966.
(28) Hamilton, P. A., unpublished results.
(29) Chapman, A. C. *Spectrochim. Acta, Part A* **1968**, *24A*, 1687. Beattie, I. R.; Livingstone, K. M. S.; Ozin, G. A.; Reynolds, D. J. *J. Chem. Soc.* **1970**, 449. Infrared absorptions recorded for P_4O_6 in solid argon in this laboratory are 953, 640, and 405 cm^{-1}.
(30) Beagley, B.; Cruickshank, D. W. J.; Hewitt, T. G.; Jost, K. H. *Trans. Faraday Soc.* **1969**, *65*, 1219.

Scheme I

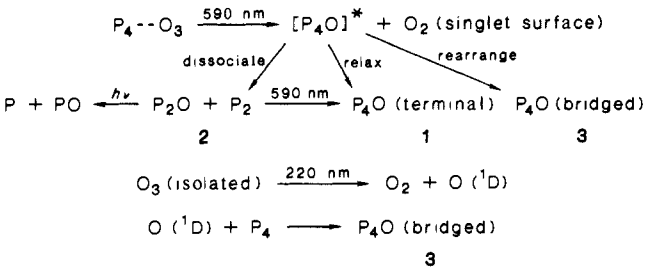

species. In particular, the 952-, 919-, and 898-cm^{-1} bands form a blue shoulder on the 856-cm^{-1} species **3** band (Figure 4) in the P–O single-bond region leading to the position, 953 cm^{-1}, of the strongest P_4O_6 absorption.[29] This evidence and the observation of mixed isotopic components in the 900-cm^{-1} region suggest that the 898-, 919-, and 952-cm^{-1} bands are due to P_xO_y species with x probably = 4 and $y \geq 2$. The near ($\pm$1-cm^{-1}) agreement with the three strongest IR bands of P_4O_6 in solid argon[29] suggests that P_4O_6 is produced in these experiments and provides further support for the identification of bridged P_4O. The 1270-cm^{-1} band is clearly in the terminal P=O stretching region, and with mixed isotopic components, this band could be due to a terminally bonded P_xO_y species with x probably = 4 and y = 2.

Note Added in Proof. Work in progress on As_4 + O reactions in this laboratory has provided evidence for linear and cyclic forms of As_2O, which invites consideration of a possible cyclic P_2O species here. MP2/6-31G*//MP2/6-31G* calculations (Davis, S. R., unpublished results), however, show that linear P_2O is more stable than the cyclic form by 10 kcal/mol. Although we cannot absolutely rule out cyclic P_2O as the source of the bands assigned above to bridged P_4O, we believe the close comparison with P_4O_6 and the ^{18}O shifts for antisymmetric and symmetric stretching modes substantiate the bridged P_4O assignment.

Mechanisms. The spectroscopic evidence for the P_4--O_3 complex, which plays an important role in the photochemistry, is primarily the broadening of P_4 and O_3 bands; in particular, the ν_1 (A_1) mode of P_4 is broadened and red shifted 6 cm^{-1} in the complex. The onset of photolysis for P_4--O_3 is in the red, based on the observation of strong product bands with 590–1000-nm radiation. This requires a specific electronic interaction between P_4 and O_3 in the complex since matrix-isolated ozone is not photodissociated by the same red light,[18] and absorption of ozone in this region is particularly weak.[27] Similar photolysis behavior was observed for the H_3P--O_3 complex.[18,25] It is generally thought[31] that the weak red absorption of ozone is due to a singlet–triplet excitation followed by dissociation to ground-state products.

$$O_3\ (S_0) + h\nu \rightarrow [O_3]^*\ (T_1) \rightarrow O_2\ (^3\Sigma_g^-) + O\ (^3P)$$

At wavelengths shorter than 590 nm in the gas phase, the products O_2 ($^1\Delta_g$) and O (^3P) are energetically possible, but the transition is still spin forbidden.[31] However, the immediate presence of a strong oxygen receptor molecule provided by the complex can increase the transition moment and may even allow the photochemical reaction to proceed on a singlet surface with the associated higher transition probability.

$$P_4\text{--}O_3\ (S_0) + h\nu \rightarrow [P_4O]^*\ (S_0) + O_2\ (^1\Delta_g)$$

The first step in the red photolysis of P_4--O_3 is to produce excited $[P_4O]^*$ (Scheme I); the matrix must quench 130 $\pm$ 10 kcal/mol from the new phosphoryl bond or terminal P_4O will dissociate most likely into P_2 + P_2O, since the heat of dissociation of P_4 to $2P_2$ is only 55 kcal/mol,[1] or rearrange to bridge-bonded P_4O. Green photolysis produced a small yield of **3** in the ozone experiments; however, full-arc irradiation gave a substantially higher yield of **3**. In the discharge experiments, P_2O was destroyed

Scheme II

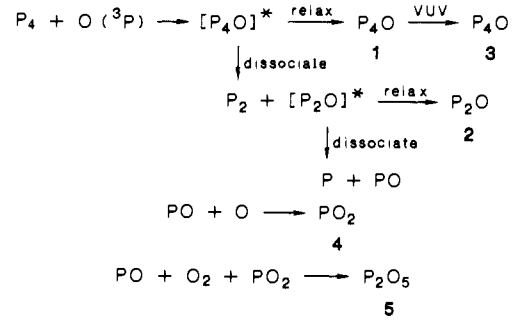

by green light, and subsequent full-arc radiation doubled the **3** bands already present from the O atom reaction. Clearly, UV radiation can dissociate isolated ozone, and the O (^1D) produced[31] can undergo insertion reactions.[32,33] It is suggested that bridged P_4O results from the diffusion and reaction of O (^1D) with P_4. A small amount of bridged P_4O was produced by red and green photolysis of the P_4--O_3 complex. It appears that energized $[P_4O]^*$ relaxes to give primarily terminal P_4O and a small amount of bridged P_4O. PO was also removed by UV photolysis, presumably due to back-reaction with P, P_2, and/or P_3 to give the bridged P_4O species.

The low-power discharge experiments gave essentially a blind discharge source of ground-state O atoms to react with P_4. Accordingly, terminal P_4O and P_2O were the major reaction products (Scheme II). On the other hand, the high-power discharge combined O atoms with vacuum ultraviolet radiation, and the P_4 reagent was mostly consumed. In this case terminal P_4O was a major product, but the photosensitive P_2O species was trapped in low yield. Bridged P_4O was also a major product along with the higher oxide species PO_2 and P_2O_5. The most likely mechanism for formation of bridged P_4O in the high-power discharge experiments is vacuum ultraviolet photochemical rearrangement of terminal to bridged P_4O although direct reaction with excited oxygen atoms cannot be ruled out.

Conclusions

Red photolysis of the P_4--O_3 complex in solid argon gave terminally bonded P_4O as the major product, which is analogous to H_3P--O_3 complex photochemistry and its H_3PO product. The P_4O species, initially formed with considerable internal energy, was relaxed by the matrix, dissociated into P_2 and P_2O, or rearranged to bridge-bonded P_4O. The terminal P_4O molecule has C_{3v} symmetry and is characterized by two modes with large ^{18}O shifts, a phosphoryl stretch at 1241 cm^{-1} and a deformation at 243 cm^{-1}, and four P–P stretching modes near P_4 values. A photosensitive molecule, probably P_2O, is formed by decomposition of P_4O and exhibits a phosphoryl stretch at 1197 cm^{-1}. These lower oxides of phosphorus have been trapped for the first time as molecular species, owing to efficient quenching of internal energy by the matrix gas during reagent condensation. Ultraviolet photolysis produced strong 856-cm^{-1} and weak 553-cm^{-1} bands in the P–O single-bond region, which are probably due to the C_{2v} bridge-bonded P_4O species.

The lower oxides P_4O and P_2O were major products of a low-power discharge oxygen reaction where ground-state O atoms in lower concentration without radiation reacted with P_4 during condensation. Photolysis again destroyed P_2O and produced bridged P_4O. Both terminal and bridged P_4O were major products of high-power discharge oxygen reaction where O atoms in higher concentration reacted with P_4 in the presence of intense vacuum ultraviolet radiation. The higher oxides PO_2 and P_2O_5 were detected as a minor products. The PO_2 molecule exhibits an isotopic triplet for ν_3 with $^{16,18}O$ and the predicted ^{18}O shift for a C_{2v} molecule with the 135° valence angle from microwave studies. The solid argon matrix moderates the reaction of O atoms

(31) Calvert, J. G.; Pitts, J. N. Jr. *Photochemistry*; Wiley: New York, 1966.

(32) Hawkins, M.; Andrews, L. *J. Am. Chem. Soc.* **1983**, *105*, 2523.
(33) Withnall, R.; Andrews, L. *J. Phys. Chem.* **1985**, *89*, 3261.

with P_4 and allows several small higher oxide species to be trapped for spectroscopic study.

Acknowledgment. We gratefully acknowledge financial support from NSF Grant CHE85-16611 and helpful discussions with P. A. Hamilton and M. E. Boyle.

Registry No. 1, 114584-25-7; **2**, 114584-26-8; **3**, 114584-27-9; **4**, 12164-97-5; **5**, 1314-56-3; PO, 14452-66-5; P_4, 12185-10-3; O, 17778-80-2; O_3, 10028-15-6; P, 7723-14-0; $^{18}O_2$, 14797-71-8.

Carbon and Proton Basicity

John I. Brauman* and Chau-Chung Han

Contribution from the Department of Chemistry, Stanford University, Stanford, California 94305-5080. *Received November 23, 1987*

Abstract: Thermodynamic basicities toward protons and methyl cations in the gas phase are compared for a variety of bases. It is shown that because the heats of formation of the corresponding neutral compounds are well correlated, the proton affinities and methyl cation affinities of many of the common bases in organic chemistry are surprisingly well correlated also.

The relationship between carbon and proton basicity has been a matter of continuing interest in chemistry.[1] Examination of this relationship has provided a number of interesting insights. The most widely cited analysis is that of Hine and Weimer[2] although numerous others have been important contributions.[3-5] Prior to Hine's work, it was generally believed that "thermodynamic affinity for carbon parallels that for hydrogen".[2] Subsequent to Hine's seminal paper, the general lore associated with this problem changed and can be summarized briefly: While there appears to be a rough correlation of carbon and proton basicity, especially within a similar series of bases, there are numerous cases where the correlation is poor, and indeed attempts to predict carbon basicity from proton basicity are likely to fail. Thus, in one of the more widely cited examples,[2,5] in aqueous solution the methyl basicity of CN^- is 10^{14} greater than that of $C_6H_5O^-$, but it is 10 times less basic toward protons.

In the process of trying to analyze nucleophilic reactivity in terms of intrinsic properties of nucleophiles and the exothermicities of their reactions, we noted that the behavior of bases in the gas phase toward protons and methyl cations is not nearly as random as might be thought, based on the above example and others like it.[6] The purpose of this paper is to point out that the thermochemistry of bases toward protons and methyl cations is, in fact, very regular and that carbon basicity can be reasonably well predicted from proton basicity.

That the correlation of proton and methyl cation basicity is roughly satisfactory can be seen in Figure 1, in which the methyl cation affinity has been plotted against the proton affinity for a wide variety of common bases.[7-10] We have made use of gas-phase values because these are a rather complete set, are probably more reliable than solution values for these purposes, cover an extremely wide range, and are free of solvation effects, thus representing intrinsic molecular behavior. Inasmuch as the entropy changes for gas-phase proton-exchange reactions are either zero or very small,[11] the use of enthalpy rather than free energy is appropriate here. In fact, equilibrium acidities of acids in solution are often strongly affected by entropy changes, owing to solvation effects, vide infra. There are indeed some substantial deviations even in the gas-phase plot, and when these are converted from energy to equilibrium constants, a comparison between some pairs of bases can produce a large difference. One of the most striking pairs is CN^- and F^-. CN^- is about 10^{13} times less basic toward protons than is F^-, but about 10 times more basic toward CH_3^+. In the gas phase, CN^- is much more basic than is $C_6H_5O^-$ toward CH_3^+ but only slightly more basic toward H^+, echoing its solution behavior.

Analysis. It is tempting to analyze Figure 1 in terms of positive deviations (mostly carbon acids) and negative deviations (mostly other first-row anions). The simple plot of methyl cation affinity vs proton affinity in Figure 1 lacks an important element, however. The essence of our analysis can be seen from eq 1 and 2, which define the proton affinity (PA) and the methyl cation affinity (MCA).

$$HA \rightarrow H^+ + A^- \qquad PA = \Delta H^\circ$$

$$PA = \Delta H_f^\circ(H^+) + \Delta H_f^\circ(A^-) - \Delta H_f^\circ(HA) \qquad (1)$$

$$CH_3A \rightarrow CH_3^+ + A^- \qquad MCA = \Delta H^\circ$$

$$MCA = \Delta H_f^\circ(CH_3^+) + \Delta H_f^\circ(A^-) - \Delta H_f^\circ(CH_3A) \qquad (2)$$

$$MCA(A^-) - PA(A^-) = \Delta H_f^\circ(CH_3^+) - \Delta H_f^\circ(H^+) - \Delta H_f^\circ(CH_3A) + \Delta H_f^\circ(HA) \qquad (3)$$

Since the heats of formation of H^+ and CH_3^+ are constants, one can see immediately from eq 3 that the relationship of proton affinities and methyl cation affinities depends only on the heats of formation of the corresponding neutrals HA and CH_3A and has nothing to do with the ions at all, either in solution or in the gas phase.[12] Moreover, if the differences between these heats

(1) For example, see: Lowry, T. H.; Richardson, K. S. *Mechanism and Theory in Organic Chemistry*, 3rd ed.; Harper and Row: New York, 1987; p 367.
(2) Hine, J.; Weimer, R. D., Jr. *J. Am. Chem. Soc.* **1965**, *87*, 3387.
(3) Hine, J. *Structural Effects on Equilibria in Organic Chemistry*; Wiley: New York, 1975; p 225.
(4) See ref 2 and 3 for some of the relevant contributions to this area.
(5) Bordwell, F. G.; Cripe, T. A.; Hughes, D. A. In *Nucleophilicity*; Harris, J. M., McManus, S. P., Eds.; Advances in Chemistry Series 215; American Chemical Society: Washington, DC, 1987; p 137.
(6) Brauman, J. I.; Dodd, J. A.; Han, C.-C. In *Nucleophilicity*; Harris, J. M., McManus, S. P., Eds.; Advances in Chemistry Series 215; American Chemical Society: Washington, DC, 1987; p 23.
(7) Heats of formation of neutrals have been taken from: Benson, S. W.; *Thermochemical Kinetics*, 2nd ed.; Wiley: New York, 1976.
(8) Bartmess, J. E.; McIver, R. T., Jr. In *Gas Phase Ion Chemistry*; Bowers, M. T., Ed.; Academic: New York, 1979; Vol. 2, Chapter 11.
(9) Methyl cation affinities have been calculated by the proton affinities and the heats of formation of the neutral proton and methyl acids, vide infra.
(10) Hydrogen (H_2) has not been included in the least-squares regression.
(11) In general the entropy change will be identical for the proton and methyl basicity, unless the rotational degrees of freedom are different for the corresponding compounds. This will occur for atomic bases or linear bases with nonlinear conjugate acids.
(12) This has been fully understood and noted before by all of the authors who have made important contributions to the area.

0002-7863/88/1510-5611$01.50/0